Biochemical and Biophysical Research Communications **286,** 1073–1081 (2001)
doi:10.1006/bbrc.2001.5523, available online at http://www.idealibrary.com on IDEAL®

Archaeoglobus fulgidus RNase HII in DNA Replication: Enzymological Functions and Activity Regulation via Metal Cofactors

Qing Chai,* Junzhuan Qiu,* Brian R. Chapados,† and Binghui Shen*,[1]
**Department of Cell and Tumor Biology, City of Hope National Medical Center, Duarte, California 91010; and*
†Department of Molecular Biology, Skaggs Institute for Chemical Biology MB4, Scripps Research Institute, 10550 North Torrey Pines Road, La Jolla, California 92037

Received August 8, 2001

RNA primer removal during DNA replication is dependent on ribonucleotide- and structure-specific RNase H and FEN-1 nuclease activities. A specific RNase H involved in this reaction has long been sought. RNase HII is the only open reading frame in *Archaeoglobus fulgidus* genome, while multiple RNases H exist in eukaryotic cells. Data presented here show that RNase HII from *A. fulgidus* (aRNase HII) specifically recognizes RNA–DNA junctions and generates products suited for the FEN-1 nuclease, indicating its role in DNA replication. Biochemical characterization of aRNase HII activity in the presence of various divalent metal ions reveals a broad metal tolerance with a preference for Mg^{2+} and Mn^{2+}. Combined mutagenesis, biochemical competitions, and metal-dependent activity assays further clarify the functions of the identified amino acid residues in substrate binding or catalysis, respectively. These experiments also reveal that Asp129 form a second-metal binding site, and thus contribute to activity attenuation.

Discontinuous DNA polymerization during lagging strand DNA synthesis is initiated by RNA primer synthesis and results in the production of Okazaki fragments consisting of covalently linked RNA and DNA. Once the Okazaki fragments are made, RNA primers have to be removed prior to ligation of nascent DNA fragments. Therefore, RNA primer removal is a critical step for the maturation of the Okazaki fragment. Failure of this process can lead to genome instability, cell growth defects or cell death (1, 2). RNase H proteins are present in all three kingdoms of living organisms. They specifically cleave the RNA portion of an RNA/DNA hybrid with limited sequence specificity (1, 2). Cleavage usually requires divalent cations, and results in products with 5′-phosphate and 3′-hydroxyl termini (1–3). *In vitro* reconstitution experiments using proteins isolated from calf thymus have convincingly demonstrated that lagging strand DNA replication requires both RNase HI (the major replicative RNase H in mammalian systems) and flap endonuclease-1 (FEN-1) activities. The mammalian RNase HI removes initiator RNA primers except for the last ribonucleotide 5′ to the RNA · DNA junction, which is removed by FEN-1 nuclease (4–8). The gene encoding this activity has been identified recently, however, more evidence is needed to determine which RNase H is involved in DNA replication in both eukaryotic and prokaryotic cells (9).

There are two major families of RNases H, type 1 and type 2, in both prokaryotic and eukaryotic cells. The type 1 family includes bacterial RNases HI, human RNase H2, and retroviral RNase H domains of reverse transcriptases. Bacterial RNases HII and HIII, archaeal RNases HII, *S. cerevisiae* RNase H(35), and the human RNases HI are type 2 enzymes (10). Although multiple *rnh* genes may exist in a single genome, there is only one active form of RNase H that is expressed in some organisms (9–13). Sequence comparison of type 1 and type 2 RNase H family members revealed low similarity. For example, there is only 17% sequence similarity between these two families in *E. coli*. This low degree of sequence similarity suggests these enzymes have differential functions within the cell, and experiments have shown that type 1 enzyme may actually function in transcription and DNA repair (14–16). Using consensus sequences of the type 1 and type 2 RNases H, we have recently scanned the several genomes, for which complete sequences are known. We and others found that only one RNase H, a type 2 RNase H, exists in the *Archaeoglobus fulgidus* genome

This work was supported by a NIH Grant CA85344 to B.H.S.
[1] To whom correspondence should be addressed. Fax: (626)-301-8972. E-mail: bshen@coh.org.

0006-291X/01 $35.00

(10), which is likely involved in DNA replication. *In vivo* experiments in other organisms have provided further evidence. A double deletion of the type 2 RNase H genes (*rnhB* and *rnhC*) in *B. subtilis*, led to cell death, indicating that this family of RNases H plays a role in DNA replication and is essential for cell growth (17). Even though deletion of the RNase HII homologue (*RNH35*) in yeast does not lead to obvious phenotypes, double deletion of *RNH35* and *RAD27* (*FEN-1* homologue) genes resulted in severe growth defects or cellular lethality, which could be rescued by plasmid-expression of the *RNH35* (18).

Structural and biochemical analysis of RNase HII from *A. fulgidus*, *M. jannaschii*, and *T. kodakaraensis* identified the active site and suggested key structural elements necessary for RNA primer removal (19–21). To provide further biochemical evidence supporting the role of this nuclease in DNA replication and experimentally test biochemical functions of the identified structural features, comprehensive site-directed mutagenesis, biochemical, and kinetic analyses were carried out in the present study. Here, we provide detailed biochemical characterization of RNase HII from *A. fulgidus* (aRNase HII). The recombinant aRNase HII is metal-dependent and specifically cleaves the RNA portion of an RNA · DNA/DNA hybrid. aRNase HII showed differential activity in the presence of metal ions such as Mg^{2+}, Mn^{2+}, Co^{2+} or Ni^{2+}. Biochemical activity assays and detailed kinetic analysis supports the proposed roles of three conserved acidic residues, D6, E7, and D101 in metal coordination at the active site. Site directed mutagenesis, and competition experiments confirm the identity of active site residues and are consistent with the role of the C-terminal conserved residues, R46, K143, R146, and Y164 in substrate binding. Finally, concentration-dependent metal ion activity assays with aRNase HII mutants support a role for Asp129 in coordinating a second metal ion which probably plays a role in regulating the enzyme activity at high metal concentrations. These results provide biochemical evidence supporting the role of aRNase H and its eukaryotic homologues in DNA replication as well as insight into the regulation and structure-function relationship of this enzyme in DNA replication.

MATERIALS AND METHODS

Materials. Chemicals were purchased from Sigma Chemical Co. (St. Louis, MO) and molecular biological reagents were from Boehringer Mannheim (Indianapolis, IN) or New England Biolabs (Beverly, MA) and were used as recommended by the manufacturers unless otherwise indicated. Plasmid DNA was purified according to the recommended midi-prep protocol from Qiagen (Santa Clarita, CA). Chromatographic materials for chelating chromatography and fast protein liquid chromatography (FPLC) were obtained from Pharmacia Biotech (Piscataway, NJ). Protein concentrations were determined by either the calculated OD_{280} value or by the Bio-Rad protein assay kit (Bio-Rad, CA). [γ-^{32}P]ATP was obtained from New England Biolabs. Oligonucleotides were synthesized on an Applied Biosystems, Inc. DNA synthesizer at the City of Hope RNA/DNA/Peptide synthesis core facility. *E. coli* RNase HI was purchased from USB corporation (Cleveland, OH). The recombinant *S. cerevisiae* RNase H(35) was the laboratory stock (18). aRNase HII and the mutant proteins were purified as previously described (19).

Site-directed mutagenesis. Plasmid pET28b-RH, containing the *Not*I-*Bam*HI fragment of aRNase H cDNA, was used as a template for mutagenesis. All of the mutants used in this study were constructed using the Quick-Change site-directed mutagenesis kit from Stratagene (La Jolla, CA). The following are the sequences of the oligonucleotides used for mutagenesis with the substituted codons underlined and names of mutants in parentheses: 5′-CTGATGAAGGCAGGCATCAACGAGGCTGGAAAGGGC (D6N); 5′-GCAGGCATCGATCAGGCTGGAAAGGGC (E7Q); 5′-CTTGGTGTGAAAAACTCCAAAAAAGCTAAGTCAG (D37N); 5′-CTTGGTGTGAAAGCCTCCAAAAAAGCTAAGTCAG (D37A); 5′-GGTGTGAAAGACGCCAAAAAGCTAAGTCAG (S38A); 5′-GTGAAAGACTCCGCAAAGCTAAGTCAGGGG (K39A); 5′-GACTCCAAAAAGGCAAGTCAGGGGAGG (L41A); 5′-CTAAGTCAGGGGGCGAGAGAGGAACTA (R45A); 5′-AGTCAGGGGAGGGCAGAGGAACTA (R46A); 5′-CCGGAAATTGCTTATGTTAACAGTCCTGATGTGATTCCC (D101N); 5′-GAGCACAAGGCGAACGAGAAGTATCCC (D129N); 5′-GAGCACAAGGCGGCCAAGTATCCC (D129A); 5′-GTAGCTGCGGCTGCAATCATCGCAAAG (S139A); 5′-CAATCATCGCAGCGGTGGAAAGGGAG (K143A); 5′-CGCAAAGGTGGAAGCGGAGCGGGAG (R146A); 5′-CGGCAGCGGCGCTGCGAGCGATCCG (Y164A); 5′-GGCTATGCGAGCGCTCCGAGGACAAG (D167A); 5′-CCGAGCTCGGTGGCAATGCGCTGGAAGACG (R188A). The mutations were verified by sequencing the plasmid DNA at the City of Hope DNA sequencing facility. Mutant protein overexpression and purification were carried out as described for the wild type aRNase HII.

Substrate preparation. The substrates used in this study are depicted in Fig. 1A. Oligoribonucleotides were 5′-end-labeled with [γ-^{32}P] ATP and T4 polynucleotide kinase. Hybridization reactions were performed in a reaction buffer (20 mM Tris, 10 mM $MgCl_2$, 25 mM NaCl) containing 100 nM labeled oligoribonucleotide and 200 nM complementary DNA (depicted as a solid line). Reactions were heated at 72°C for 5 min, then slowly cooled down to room temperature for oligonucleotide annealing.

RNase H activity assay. RNase H assays were performed using standard reaction conditions (50 mM Tris–HCl, pH 8.0, 1 mM $MgCl_2$, 1.5 μM BSA, 5 mM β-mercaptoethanol) containing 0.1 μM of substrate unless otherwise specified. Enzyme concentrations used for a typical assay ranged from 0.1 nM to 10 nM. All reactions were incubated at 30°C for specified time intervals and quenched with an equal volume of the stop solution (USB, Cleveland, OH). A base hydrolysis ladder was prepared by incubation of 5′-end-labeled RNA · DNA oligos at 90°C for 5 min in 100 mM $NaCO_3$ (pH 9.0).

Steady-state enzyme kinetics. Initial velocity was determined by measuring product intensities over a range of substrate concentrations on a 15% denaturing polyacrylamide gel using a phosphorimager and the software "Lab gel" (Molecular Dynamics, Sunnyvale, CA). Kinetic reactions were set up with excess amount of substrates and a low enzyme concentration. The velocity was expressed as the rate of converted substrate concentration (nM) over time (min). One unit of enzyme activity is defined as the amount of enzyme producing 1 μmol of product per minute. The specific activity was defined as the enzymatic activity per milligram of protein. Enzymatic hydrolysis of the substrate with the enzyme follows the Michaelis–Menten kinetics. The kinetic parameters, K_m and V_{max} were determined using the Eadie–Scatchard or Lineweaver–Burk plots. The data from multiple assays was analyzed using linear regression methods and CricketGraph software (Cricket Software, Philadelphia, PA). A linear plot produces a slope of $-1/K_m$ and an X-intercept of V_{max}.

Competition assay. Using standard RNase H assay conditions, 4 nM of WT aRNase HII was incubated with 0 to 3200 nM of mutant proteins and 200 nM 18 mer RNA · DNA/DNA substrates for 8 min. An assay containing 4 nM WT aRNase HII without any mutant protein was performed as a control. Samples were then analyzed using polyacrylamide gel electrophoresis and the phosphorimager.

Circular dichroism measurements. Circular dichroism (CD) data were collected on a J-600 spectropolarimeter from Japan Spectroscopic Co., Ltd. (Tokyo, Japan). The far-UV (200–250 nM) CD spectrum was obtained at 25°C using a solution containing 0.24 mg/mL enzyme, 20 mM Sodium Phosphate buffer (pH 7.5) in a 2-mm pathlength cuvette. CD data were analyzed using J-600 for Windows (Jasco, Tokyo, Japan).

RESULTS AND DISCUSSION

Substrate specificity of aRNase HII compared to S. cerevisiae RNase H(35) and E. coli RNase HI. To examine how aRNase HII hydrolyzes oligomeric ribonucleotide substrates, four substrates were employed (Fig. 1A): The first two substrates, Q18 and Q1, mimic an Okazaki fragment. They are composed of varying lengths of RNA (9 bp and 21 bp respectively), covalently bound to deoxyribonucleotides and duplexed with DNA. The third substrate is a 25 bp RNA/DNA hybrid (Q2), which is a traditional RNase H substrate. The fourth is a 29-bp DNA · RNA · DNA/DNA substrate (Q3), used to test the ability to excise the ribonucleotides that have been misincorporated into DNA (8). All substrates were ^{32}P-labeled at the 5′ end of the RNA strand to allow identification by denaturing SDS–PAGE. aRNase H was purified to a near homogeneity using a method that takes advantage of thermostability of archaebacterial proteins. Two additional enzymes, *S. cerevisiae* RNase H(35) and *E. coli* RNase HI were included in these experiments to allow comparison of aRNase HII substrate specificity with previously characterized enzymes. The results of the activity assays are shown in Fig. 1B.

All three enzymes cleaved the 25-bp RNA/DNA hybrid (Q2) at multiple sites (Fig. 1B), indicating that aRNaseHII cleaves RNA/DNA in a sequence-independent manner. When the model Okazaki substrates were examined, aRNase HII cleaved the 37-mer RNA · DNA/DNA substrate (Q1) at several sites, most preferably at c20 and weakly at a9, a8, and a6. It specifically cleaved the 18 mer RNA · DNA/DNA substrate (Q18) at c8 and weakly at g7 and u6. *S. cerevisiae* RNase H(35) showed a unique cleavage site at c20 of the substrate Q1. *E. coli* RNase HI cleaved Q1 at a7, a8 and weakly at c6 and Q18 at a5 and a4. Furthermore, in the absence of complementary DNA, the chimeric RNA · DNA strand was not cleaved by aRNase HII (data not shown). These experiments demonstrate that RNase H is a structure-specific endonuclease. When the 29-bp DNA · RNA · DNA/DNA substrate (Q3) was used, *E. coli* RNase HI cleaved the substrate in the middle of the tetra-adenosine (a15-a16) region, consistent with what was previously reported using the same substrate (22–24). In contrast, aRNase HII and the *S. cerevisiae* RNase H(35) specifically cleaved Q3 at the phosphodiester bond between the third and fourth adenosines (a16–a17). Type 2 RNase H enzymes from calf thymus (7, 8), *S. cerevisiae* (19), the archaeon, *Pyrococcus kodakaraensis* (25) and *B. subtilis* (24) have been shown to cleave 5′ of the last ribonucleotide at the RNA · DNA junction, but not at the junction between RNA and DNA. Our results demonstrate that aRNase HII also possesses such catalytic specificity for model Okazaki fragments (Q1 and Q18), indicating the potential for coordination with the FEN-1 nuclease to remove the ribonucleotide during DNA replication.

Metal-dependence of enzyme activity. aRNase HII was shown to be a strictly metal-dependent nuclease. It exhibited activity in the presence of Mg^{2+}, Mn^{2+}, Co^{2+} or Ni^{2+}, whereas no activity was observed in the absence of these metal ions (Fig. 2A). Little activity was detected in the presence of other metals including Co^{3+}, Cu^{2+}, Zn^{2+}, and Ca^{2+}. In contrast to *E. coli* RNase HII, whose activity is dependent on the Mn^{2+} ion only (25), aRNase HII exhibited rather broad metal ion specificity, which is similar to *P. kodakaraensis* RNase HII ($RNase\ HII_{pk}$) (24). The different metal specificity between eubacterial and archaebacteral RNases H may be a consequence of the different environments in which they are found.

The dependence of the aRNase H activity on the divalent cation concentrations was further analyzed for Mg^{2+}, Mn^{2+}, Co^{2+}, and Ni^{2+}, respectively. Optimal enzyme activities in the presence of Mg^{2+} or Mn^{2+} are 3- to 7-fold higher than that with the other two metals. The optimum concentration of Co^{2+} or Ni^{2+} needed for aRNase HII activity is 1 mM (Figs. 2D and 2E). Though aRNase HII can utilize both Mg^{2+} and Mn^{2+}as cofactors, there is a drastic difference in the concentration needed for optimal activity. Maximum aRNase HII activity was observed at concentrations of 6.4 mM Mg^{2+} and at 50 μM Mn^{2+} (Fig. 2B and 2C). The specific activity determined in the presence of 50 μM Mn^{2+} was 35% of that determined in the presence of 6.4 mM Mg^{2}. Furthermore, when Mn^{2+} was added in the presence of 1.6 mM Mg^{2+}, the enzyme activity increased gradually as the Mn^{2+} concentration reached 50 μM and decreased after that point. At equal concentrations of Mn^{2+} and Mg^{2+} (1.6 mM), the enzyme activity was reduced 10-fold compared to the activity in the presence of only Mg^{2+} (Fig. 2F). Enzyme activity did not increase by the addition of Mn^{2+} when Mg^{2+} was present at the optimal concentration (6.4 mM) (Fig. 2F).

The optimal concentration needed for activity is different, especially for Mg^{2+} (6.4 mM) and Mn^{2+} (50 μM). It appears that the enzyme has stronger binding affinity with Mn^{2+}, whereas the maximal activity with Mg^{2+} is 2-fold higher than that stimulated by Mn^{2+}. This

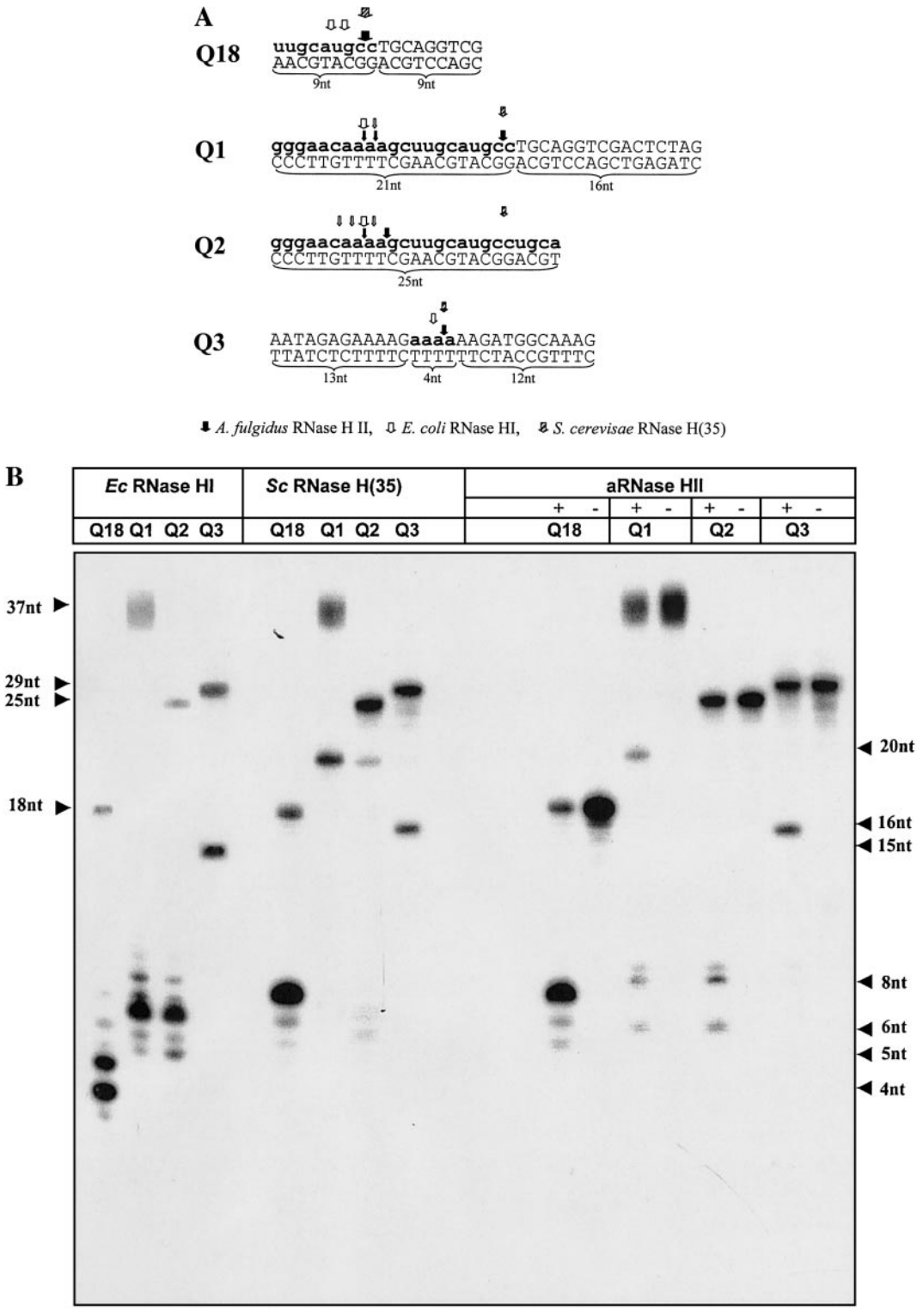

FIG. 1. Cleavage specificity of the purified recombinant aRNase HII. (A) Graphical representation of sites and extents of cleavages in substrates by RNases H. Cleavage sites in the substrates Q18, Q1, Q2, and Q3 with aRNase HII, *E. coli* RNase HI, and *S. cerevisiae* RNase H(35) are denoted with different arrows. Deoxyribonucleotides are denoted with uppercase letters, while ribonucleotides are denoted with lowercase letters in bold. The complementary DNA strand is shown under the RNA (·DNA) strand. The asterisk indicates the radioactively labeled site. (B) Denaturing polyacrylamide gel analysis of cleavage reactions. Hydrolysis of substrates (Q18, Q1, Q2, and Q3) with aRNase HII, *E. coli* RNase HI, and *S. cerevisiae* RNase H(35) was carried out at 30°C for 10 min under the conditions described under Materials and Methods. The hydrolysates were separated on a 15% polyacrylamide gel containing 7 M urea. The similar assays with the four substrates omitting enzyme (−) were run as controls. Based on base-hydrolyzed RNA ladders, sizes of the major substrates (left) and their cleavage products (right) are indicated.

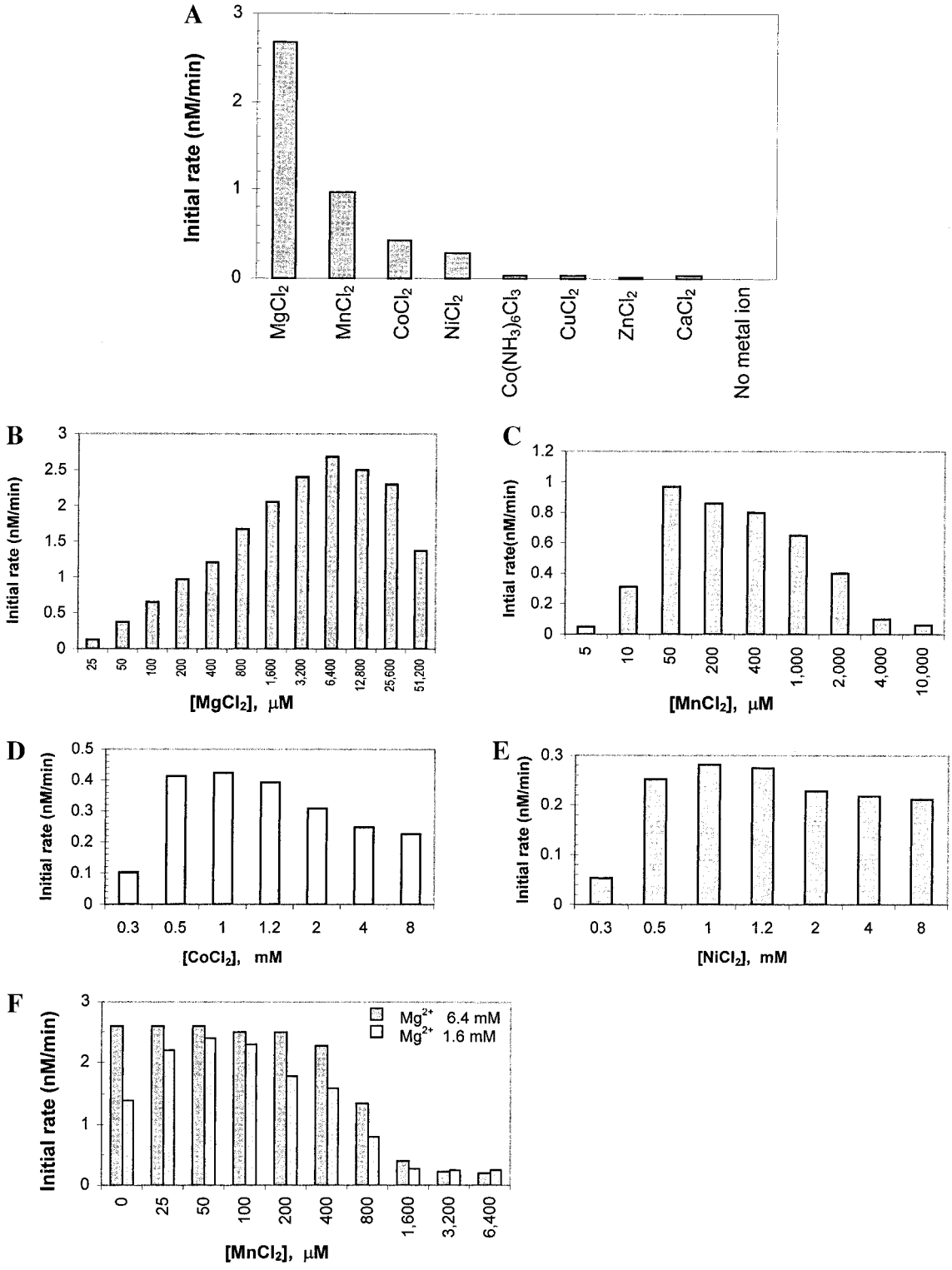

FIG. 2. Effects of metal ions on RNase H activity. Assays were performed at indicated divalent cation concentrations in 50 mM Tris–HCl, pH 8.0, 50 mM NaCl, 1.5 μM BSA, 5 mM β-mercaptoethanol, 100 nM RNA/DNA hybrid substrate, and 1 nM enzyme at 30°C. The activity was measured as initial rate. (A) Metal dependence of aRNase HII activity. The metal concentration used in the assay was 6.4 mM for Mg^{2+}, 50 μM for Mn^{2+}, 2 mM for Co^{2+}, and Ni^{2+}, and 2 mM for all the other metal ions. (B) [Mg^{2+}]-dependent aRNase HII activity. (C) [Mn^{2+}]-dependent aRNase HII activity. (D) [Co^{2+}]-dependent aRNase HII activity. (E) [Ni^{2+}]-dependent aRNase HII activity. (F) Effects of Mn^{2+} on RNase HII activity in the presence of 6.4 or 1.6 mM Mg^{2+}.

may result from inherent differences in the manner through which these cations contribute to catalysis. Differential activities with the metal cations have been observed for other RNases H as well. RNase HII from *B. subtilis* and *E. coli* showed a preference for Mn^{2+} (23, 25), whereas RNase HIII of *B. subtilis* was Mg^{2+}-dependent (23). RNase HII from another hyperthermophilic archaea, *P. kodakaraensis* preferred Co^{2+} for activity and could also tolerate Mg^{2+}, Mn^{2+} and Ni^{2+} (25). Metal ions play an important role in either stabilizing the enzyme-substrate complex or in activating H_2O molecules to facilitate hydrolysis. It may also regulate the enzyme activity upon its binding of an additional metal. The diversity of metal ion usage by type 2 RNase H may be a survival strategy of an organism, and an indication of the role of the RNase H in DNA replication.

Identification of conserved residues necessary for substrate cleavage or binding. To identify key structural elements responsible for metal coordination, formation of the catalytic center, and substrate binding, and enzyme activity regulation, the amino acid sequence of aRNase HII was compared with homologues from archaea, eucarya, and bacteria. The four motifs (I to IV), which are highly conserved in various type 2 RNase H sequences (9, 23–26), exist in the aRNase HII sequence (Fig. 3A). Within these four conserved motifs, there are five acidic residues (D or E) and six positively charged or aromatic residues (R, K, or Y), which are conserved in at least five out of seven homologues of the type 2 RNases H. Two more charged residues are also conserved outside of these four motifs (D101 and R188). We performed site-directed mutagenesis on the additional conserved residues in aRNase HII as indicated in Fig. 3A. Substitutive residues (alanine, asparagine, or glutamine) were chosen to minimize possible conformational changes caused by the replacement. All mutant proteins were overexpressed and purified to homogeneity. The enzymatic activities of mutants were determined using the 18 mer RNA · DNA/DNA substrate (Q18) and were compared to the wild-type activity (Figs. 3B and 3C).

Of the highly conserved residues that we selected, mutations at Ser38, Lys39, Leu41, Arg45, Ser139, and Asp167 did not significantly affect the enzyme activity. Conversion of Asp6 to Asn, Glu7 to Gln, or Asp101 to Asn almost completely inactivated the enzyme, suggesting that these carboxylic acid groups of D6, E7, and D101 are essential for catalysis. This is probably due to the disruption of enzyme active center and the disordered metal ion coordination. Co(III) containing crystals of aRNase HII suggest that the metal ion is coordinated by D6 and D101 (19). Structural superimposition of aRNase HII and *E. coli* RNase HI resulted in a near overlap of two metal-binding ligands, D6 and D101 in aRNase H compared to D10 and D70 in *E. coli* RNase HI (19, 27–29). Though the invariant acidic residue, E7, is 5 Å away from the cognate residue in *E. coli* RNase HI, the severe defect of the enzyme activity caused by the E7Q mutation indicates that E7, together with D6 and D101 forms a catalytic triad. Despite poor sequence identity, the similarity of the active site environment observed in the three-dimensional structures between aRNase HII and *E. coli* RNase HI suggests an analogous catalytic mechanism for the degradation of RNA substrates. More recent crystal structural and mutational analysis of RNase HII from *P. kodakaraensis* KOD1 indicated that an additional conserved residue H132 (corresponds to H126 in aRNase HII) plays a role in active center of the enzyme (21). In addition, the mutant D37N retained some activity, substitution of D37 with alanine dramatically decreased the enzymatic activity. Conversely, the D129N mutant exhibited decreased activity (29% of the wild type), whereas the D129A mutant retained 60% of the wild type enzyme activity. The four mutant proteins, D37N, D37A, D129N and D129A, all showed circular dichroism (CD) spectra with a strong α-helical character which were superimposable with that of the wild type enzyme (Data not shown). Hence, no gross structural rearrangements resulted from the mutation of Asp to Asn or Ala.

Interestingly, individual mutations R46A, K143A, R146A, and Y164A, resulted in a 3 to 20-fold decrease in enzyme activity, which was attributed to loss of substrate binding capability (19). A double mutation of Lys143 and Arg146 (DB), and a triple mutation of Lys143, Arg146, and Tyr164 (TP) caused the enzymatic activity to approach zero. The cumulative effects of simultaneous mutation of several basic residues support the putative structural role for these residues in substrate binding. The principal substrate-binding site is a cluster of lysine residues that interact with the phosphates of the substrates (20). The interaction of the binding surface of the enzyme and substrate is believed to occur within the minor groove (28). The conserved basic residues, which we identified, are distributed within or around the substrate-binding groove of aRNase HII observed in the crystal structure. The positively charged side chains of R46, K143 penetrate into the substrate-binding groove. These residues together with another polar residue Q43 define a "phosphate ruler" that could confer A-form nucleic acid binding specificity via charge complementation to the phosphate backbone (19). Additionally, R146 and Y164 likely aid in positioning or recognizing of a RNA/DNA duplex by interacting with negatively charged phosphate groups. This result is also consistent with the fact that deletion of the alpha 9 helix in KOD1 RNase H seriously affects the ability of the enzyme to bind substrate (21).

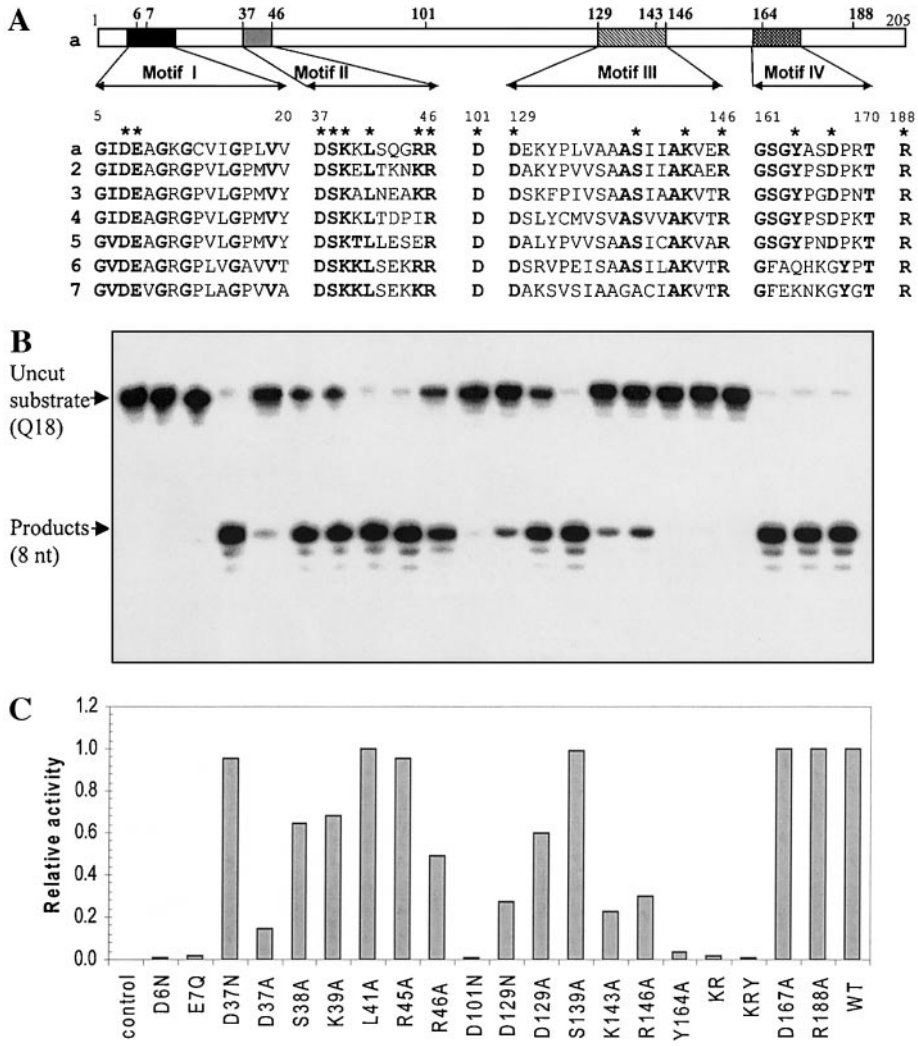

FIG. 3. (A) Schematic organization of aRNase HII. Four blocks denote the ranges of the four conserved motifs (I, II, III, and IV), which were identified by sequence alignment of the type 2 RNase H homologues from eubacteria, archaebacteria, and eukaryotes. Sequences corresponding to the four motifs are listed below with aRNase HII sequence on the top (a). Identical or similar amino acid residues in at least 5 out of 7 sequences are shown in bold. Numbering of amino acids above the alignment corresponds to the sequence of aRNase HII. Asterisks indicate the amino acid residues selected for mutagenesis in aRNase HII. The functionally significant residues that we found by site-directed mutagenesis were represented in amino acid numbers on top of the schematic bar. The homologous sequences are: a, *A. fulgidus* (GenBank AE001062); 2, *M. jannaschii* (PIR G64316); 3, *S. cerevisiae* (EMBL Z71348); 4, *C. elegans* (EMBL Z66524); 5, *H. sapiens* (EMBL Z97029); 6, *E. coli* (GenBank U70214); 7, *B. subtilis* (EMBL Z75208). (B) Cleavage capacity of mutant aRNases HII with 18-mer RNA · DNA/DNA duplex substrate. The radioactive image of urea polyacrylomide gel separation of aRNase H-digested Q18 RNA · DNA/DNA substrate is shown. Enzymatic activities of mutant aRNases HII were determined at 30°C for 10 min in 10 mM Tris–HCl (pH 8.0) containing 50 mM NaCl, 1.5 μM BSA, 5 mM β-mercaptoethanol, and 2 nM mutant aRNases HII individually using the 18-mer RNA · DNA/DNA duplex substrate (Q18). Arrows indicate the sizes of the substrates and the cleavage products. Mutational data for D6N, E7Q, D101N, and D129N has been reported in the Ref. (20). (C) Ratios of the products produced by mutant enzymes to that of the wild type.

Kinetic analysis of the wild type and mutant aRNase HII. Kinetic parameters of the mutant proteins with detectable activities were determined using the 18-mer RNA · DNA/DNA hybrid substrate (Q18). The kinetic parameters of mutant proteins relative to the wild-type enzyme are shown in Table 1. The K_m values of mutant proteins, D37N, D37A, D129N, and D129A, varied slightly from 0.7- to 2.2-fold of the wild type value. These four mutants showed reduced k_{cat} value, with the lowest being 4% of the wild type value. In contrast, the mutations R46A, K143A, R146A, and Y164A resulted in a significantly increased K_m, while the catalytic rate constants of these mutants remained within 1.6-fold of the wild type value, indicating an involvement in substrate binding.

Suppression of wild type enzyme by RNase HII mutants. The mutants provide us with a tool to further analyze the roles of the amino acid residues important for aRNase HII catalysis. To clarify the roles of the

TABLE 1

Kinetic Parameters of Wild-Type and Mutant aRNase HII Proteins with Detectable Activities

aRNase HII proteins	Relative K_m	Relative k_{cat}
Wild type	1.0	1.0
D37N	1.5	0.4
D37A	0.8	0.05
R46A	60.0	1.3
D129N	0.7	0.2
D129A	2.2	0.3
K143A	31.3	1.5
R146A	26.7	1.4
Y164A	44.7	1.6

Note. The kinetic parameters were determined from the Lineweaver–Burk plots. The measurement of the activity was performed using the Q18 hybrid as a substrate. Relative values were calculated by dividing the values for the mutant proteins by the values for the wild-type protein.

identified residues in catalysis, we experimentally tested if these mutants can compete with the wild type enzyme for the substrate and therefore suppress wild type enzyme activity. The results are shown in Fig. 4. With the increasing concentrations of mutants, D6N, E7Q, or D101N, the cleavage activity of the wild-type enzyme was dramatically suppressed. In contrast, increasing concentrations of mutants R46A, K143A, R146A, or Y164A, did not affect the wild-type cleavage activity. These data indicate that the mutants, D6N, E7Q and D101N, are dominant-negative. Their substrate binding ability is intact while their catalytic activity is lost. The suppression of the wild type enzyme activity may result from the competition for the free substrate by these mutants. However, the partially active mutants, R46A, K143A, R146A, and Y164A, along with the double and triple mutants (DB and TP) had little effect on wild type enzyme activity, supporting the role of these residues in substrate binding. Taking all these data together, we conclude that D6, E7, D37, D101 and D129 are candidate metal ligands and R46, K143, R146 and Y164 contribute to substrate binding or recognition.

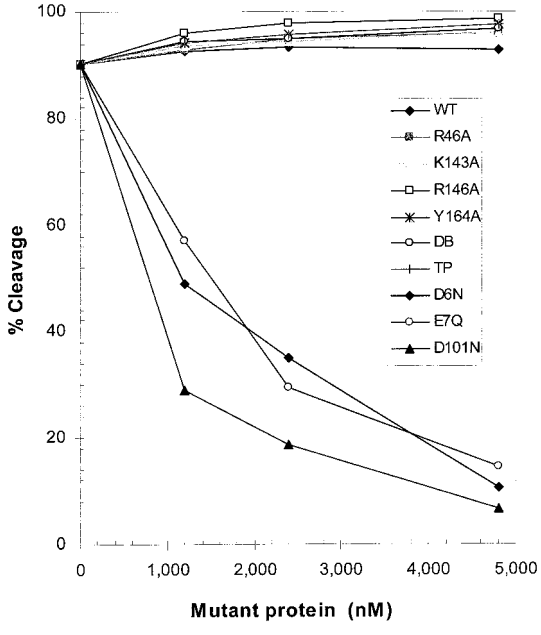

FIG. 4. The ability of mutant enzymes to suppress the wild-type aRNase HII activity. Activities of the wild-type aRNase HII were measured as a function of increasing concentrations of different mutant proteins. In a standard RNase H assay, 4 nM of WT aRNase HII was incubated with increasing amount of mutant proteins at 30°C for 8 min. The total activity was observed as percent cleavage of the 18-mer RNA · DNA/DNA substrates (Q18). The same assay with 4 nM WT enzyme omitting mutant protein was included as control (100% cleavage).

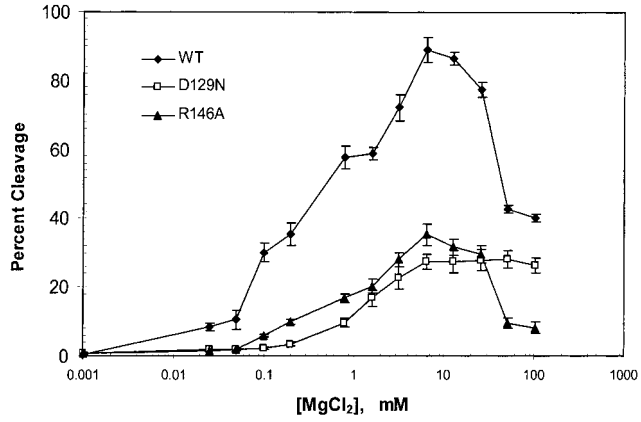

FIG. 5. Activities of wild-type aRNase HII and mutants, D129N and R146A, as a function of varying concentrations of $MgCl_2$. Assays were performed in 10 mM Tris–HCl (pH 8.0), 50 mM NaCl, 1.5 μM BSA, 5 mM β-mercaptoethanol, 100 nM Q18 RNA · DNA/DNA hybrid substrate with 1 nM enzyme at 30°C with the indicated $MgCl_2$ concentrations. Data points are the average of at least three assays with the standard deviation indicated by error bars.

D129 may participate in the second metal binding for activity inhibition. Recently a new model called the "activation/attenuation" model was proposed to explain how members of the RNase H family use active-site metal(s) for catalysis. This model was based on the study of *E. coli* RNase HI, where it was determined that mutation of the conserved residue Asp134, resulted in a partial loss of enzyme inhibition normally observed at high Mn^{2+} concentration. This finding led to the proposal that one metal is required for enzyme activation while binding of a second metal is inhibitory (30, 31). Because of the similar position and environment of Asp129 in aRNase HII to Asp134 in *E. coli* RNase HI, we tested whether the D129N RNase HII mutant would be inhibited at a high Mg^{2+} concentrations. Unlike the wild type enzyme, which shows strong inhibitory effect at a concentration greater than 6.4 mM Mg^{2+}, the inhibitory effect was not observed for the D129N mutant at even 100 mM Mg^{2+} (Fig. 5).

Although the D129A mutant has a lower basal activity rate, another mutant, R146A, with a similar basal activity exhibited a similar activation/inhibition pattern to that of wild type enzyme. These results suggest that D129 may be important for forming an inhibitory metal binding site in enzyme activity attenuation.

ACKNOWLEDGMENTS

The authors thank Y. Qian, X. Li, G. Frank, and other members in the Shen's laboratory for their technical assistance and stimulating discussions during the course of this study. We also thank M. Sherman and L. Zheng for the training to use the circular dichroism and T. LeBon, S. Novak, S. Kane, D. Thrower, and P. Wu for their critical reading of the manuscript.

REFERENCES

1. Crouch, R. J., and Dirksen, M. L. (1982) Ribonucleases H. *In* Nucleases (Linn, S. M., and Roberts, R. J., Eds.), pp. 211–241, Cold Spring Harbor Laboratory Press, Plainview, NY.
2. Crouch, R. J. (1990) Ribonuclease H: From discovery to 3D structure. *New Biol.* **2,** 771–777.
3. Stein, H., and Hause, N. P. (1969) Enzyme from calf thymus degrading the RNA moiety of DNA-RNA hybrids: effect on DNA-dependent RNA polymerase. *Science* **166,** 393–395.
4. Waga, S., and Stillman, B. (1994) Anatomy of a DNA replication fork revealed by reconstitution of SV40 DNA replication *in vitro*. *Nature* **369,** 207–212.
5. Waga, S., Bauer, G., and Stillman, B. (1994) Reconstitution of complete SV40 DNA replication with purified replication factors. *J. Biol. Chem.* **269,** 10923–10934.
6. Turchi, J. J., Huang, L., Murante, R. S., Kim, Y., and Bambara, R. A. (1994) Enzymatic completion of mammalian lagging-strand DNA replication. *Proc. Natl. Acad. Sci. USA* **91,** 9803–9807.
7. Huang, L., Kim, Y., Turchi, J. J., and Bambara, R. A. (1994) Structure-specific cleavage of the RNA primer from Okazaki fragments by calf thymus Rnase HI. *J. Biol. Chem.* **269,** 25922–25927.
8. Murante, R. S., Henricksen, L. A., and Bambara, R. A. (1998) Junction ribonuclease: An activity in Okazaki fragment processing. *Proc. Natl. Acad. Sci. USA* **95,** 2244–2249.
9. Frank, P., Braunshofer-Reiter, C., Wintersberger, U., Grimm, R., and Busen, W. (1998) Cloning of the cDNA encoding the large subunit of human RNase HI, a homologue of the prokaryotic RNase HII. *Proc. Natl. Acad. Sci. USA* **95,** 12872–12877.
10. Ohtani, N., Haruki, M., Morikawa, M., and Kanaya, S. (1999) Molecular diversities of RNases. *J. Biosci. Bioeng.* **88,** 12–19.
11. Frank, P., Braunshofer-Reiter, C., and Wintersberger, U. (1998) Yeast RNase H(35) is the counterpart of the mammalian RNase HI, and is evolutionarily related to prokaryotic RNase H. *FEBS Lett.* **421,** 23–26.
12. Frank, P., Braunshofer-Reiter, C., Poltl, A., and Holzmann, K. (1998) Cloning, subcellular localization and functional expression of human RNase HII. *Biol. Chem.* **379,** 1407–1412.
13. Itaya, M. (1990). Isolation and characterization of a second RNase H (RNase HII) of *Escherichia coli* K-12 encoded by the rnhB gene. *Proc. Natl. Acad. Sci. USA* **87,** 8587–8591.
14. Busen, W. (1977) Ribonuclease H levels during the response of bovine lymphocytes to concanavalin A. *Eur. J. Biochem.* **255,** 9434–9443.
15. Ogawa, T., and Okazaki, T. (1984) Function of RNase H in DNA replication revealed by RNase H defective mutants of *Escherichia coli*. *Mol. Gen. Genet.* **193,** 231–237.
16. Arudchandran, A., Cerritelli, S., Narimatsu, S., Itaya, M., Shin, D. Y., Shimada, Y., and Crouch, R. (2000) The absence of ribonuclease H1 and H2 alters the sensitivity of *Saccharomyces cerevisiae* to hydroxyurea, caffeine and ethyl methanesulphonate: implicationd for roles of RNases H in DNA replication and repair. *Genes Cells* **5,** 789–802.
17. Itaya, M., Omori, A., Kanaya, S., Crouch, R. J., Tanaka, T., and Kondo, K. (1999) Isolation of RNase H genes that are essential for growth of *Bacillus subtilis* 168. *J. Bacteriol.* **181,** 2118–2123.
18. Qiu, J., Qian, Y., Frank, P., Wintersberger, U., and Shen, B. (1999) *Saccharomyces cerevisiae* RNase H(35) functions in RNA primer removal during lagging-strand DNA synthesis, most efficiently in cooperation with Rad27 nuclease. *Mol. Cell. Biol.* **19,** 8361–8371.
19. Chapados, B. R., Chai, Q., Hosfield, D. J., Shen, B., and Tainer, J. A. (2001) Structural biochemistry of a type 2 RNase H: RNA primer recognition and removal during DNA replication. *J. Mol. Biol.* **307,** 541–556.
20. Lai, L., Yokota, H., Hung, L. W., Kim, R., and Kim, S. H. (2000) Crystal structure of archaeal RNase HII: A homologue of human major RNase H. *Structure* **8,** 897–904.22.
21. Muroya, A., Tsuchiya, D., Ishikawa, M., Haruki, M., Morikawa, M., Kanaya, S., and Morikawa, K. (2001) Catalytic center of an archaeal type 2 ribonuclease H as revealed by X-ray crystallographic and mutational analyses. *Protein Science* **10,** 707–714.
22. Hogrefe H. H., Hogrefe, R. I., Walder, R. Y., and Walder, J. A. (1990) Kinetic analysis of *Escherichia coli* RNase H using DNA-RNA-DNA/DNA substrate. *J. Biol. Chem.* **265,** 5561–5566.
23. Ohtani, N., Haruki, M., Morikawa, M., Crouch, R. J., Itaya, M., and Kanaya, S. (1999) Identification of the genes encoding Mn^{2+}-dependent RNase HII and Mg^{2+}-dependent RNase HIII from *Bacillus subtilis:* Classification of RNases H into three classes. *Biochemistry* **38,** 605–618.
24. Haruki, M., Hayashi, K., Kochi, T., Muroya, A., Koga, Y., Morikawa, M., Imanaka, T., and Kanaya, S. (1998) Gene cloning and charaterization of recombinant RNase HII from a hyperthermophilic archaeon. *J. Bacteriol.* **180,** 6207–6214.
25. Ohtani, N., Haruki, M., Muroya, A., Morikawa, M., and Kanaya S. (2000) Characterization of ribonuclease HII from *Escherichia coli* overproduced in a soluble form. *J. Biochem.* **27,** 895–899.
26. Zhang, Y. B., Ayalew, S., and Lacks, S. A. (1997) The rnhB gene encoding RNase HII of *Streptococcus pneumoniae* and evidence of conserved motifs in eucaryotic genes. *J. Bacteriol.* **179,** 3828–3836.
27. Katayanagi, K., Miyagawa, M., Matsushima, M., Ishikawa, M., Kanaya, S., Ikehara, M., Matsuzaki, T., and Morikawa, K. (1990) Three dimensional structure of RNase H from *E. coli*. *Nature* **347,** 306–309.
28. Yang, W., Hendrickson, W. A., Crouch, R. J., and Satow, Y. (1990) Structure of ribonuclease H phased at 2A resolution by MAD analysis of the selenomethionyl protein. *Science* **249,** 1398–1405.
29. Kanaya, S., Kohara, A., Miura, Y., Sekiguchi, A., Iwai, S., Inoue, H., Ohtsuka, E., and Ikehara, M. (1990) Identification of the amino acid residues involved in an active site of *Escherichia coli* ribonuclease H by site-directed mutagenesis. *J. Biol. Chem.* **265,** 4615–4621.
30. Keck, J. L., Goedken, E. R., and Marqusee, S. (1998) Activation/attenuation model for RNase H. A one-metal mechanism with second-metal inhibition. *J. Biol. Chem.* **273,** 34128–34133.
31. Goedken, E. R., and Marqusee, S. (2001) Co-crystal of *Escherichia coli* RNase HI with Mn^{2+} ions reveals two divalent metals bound in the active site. *J. Biol. Chem.* **276,** 7266–7271.